THEORETICAL AND EXPERIMENTAL STUDY OF LIGHT SHIFT IN A CPT-BASED RB VAPOR CELL FREQUENCY STANDARD

M. Zhu and L. S. Cutler
Agilent Laboratories
3500 Deer Creek Rd., Palo Alto, CA 94304, USA

Abstract

One of the important subjects in coherent-population-trapping-based (CPT-based) vapor cell frequency standards is the light shift (ac Stark shift). We calculate the light shift using a numerical method and perturbation approximation. Experimentally, we measure light shift using a pair of phase-locked diode lasers as well as a frequency-modulated diode laser. There is good agreement between theory and experiment. A method of controlling light shift in CPT-based frequency standards is proposed and implemented in Agilent Laboratories. The short-term stability of our CPT-based rubidium vapor cell frequency standard is measured as $1.3\times10^{-12}\,\tau^{-1/2}$ ***, which is limited by the phase noise of the reference local oscillator used.***

I. INTRODUCTION

Since it was observed [1] and explained theoretically,[2, 3] coherent population trapping (CPT) has been found in many applications.[4 - 10] Its application in atomic frequency standards has also attracted a lot of attention.[5, 11 - 13] In a CPT-based vapor cell atomic frequency standard, the potential elimination of the microwave excitation [4, 5] promises a smaller and less expensive device. However, the light shift (ac Stark shift) in CPT-based atomic frequency standards is of great importance. Here we present our calculations and experimental measurements of the light shift in a CPT-based ^{87}Rb vapor cell frequency standard. Based on the calculations, we also show that the light shift in CPT-based atomic frequency standards can be controlled, or ultimately eliminated.

II. REVIEW OF THE CONCEPTS

The light shift (ac Stark shift) is the energy level shift that originates from the interaction between the atom and the applied ac electromagnetic field.[14] Fig. 1(a) shows a two-energy-level atom interacting with a single frequency laser field with a Rabi frequency Ω, and a detuning $\Delta \equiv \omega_L - \omega_0$. This resembles part of a simple optical pumping scheme used in atomic frequency standards. Since the Rabi frequency Ω is usually much less than the spontaneous decay rate of the upper state $|e\rangle$, the light shift can be calculated using perturbation approximation.[15, 16] The perturbation approximation can be readily expanded to include the case involving multiple atomic energy levels and multiple laser frequency components. Alternatively, the light shift can be obtained using the concept of the dressed state,[14, 17] which gives a more intuitive physical explanation. The energy level shift (light shift) of the lower state $|g\rangle$ is given by

$$\delta E_g = \frac{\hbar}{4}\frac{|\Omega|^2 \Delta}{\Delta^2 + \gamma^2} \tag{1}$$

where γ is the decay rate of the excited state $|e\rangle$. The light shift in Eq. (1) has a dispersion line shape, the magnitude of which decreases inversely proportional to the detuning Δ when the detuning is large.

Coherent population trapping can happen in a three-energy-level atom interacting with a dual-frequency laser field as shown in Fig. 1(b). The two transitions from $|g_i\rangle$ to $|e\rangle$ driven by laser frequency ω_{Li} (i = 1, 2) are essential for CPT generation, so we call them CPT-generating interactions. In Fig. 1(b), we temporarily exclude the interaction of the frequency component with frequency ω_{L1} (ω_{L2}) and induced electric dipole moment between the upper state $|e\rangle$ and the lower state $|g_2\rangle$ ($|g_1\rangle$) in order to keep the following analysis simple. Using the rotating wave approximation (RWA), one can write the interaction Hamiltonian as

$$\hat{H}_I = \frac{1}{2}\hbar\Omega_1 e^{-i\omega_{L1}t}|e\rangle\langle g_1| + \frac{1}{2}\hbar\Omega_1^* e^{i\omega_{L1}t}|g_1\rangle\langle e| + \frac{1}{2}\hbar\Omega_2 e^{-i\omega_{L2}t}|e\rangle\langle g_2| + \frac{1}{2}\hbar\Omega_2^* e^{i\omega_{L2}t}|g_2\rangle\langle e| \tag{2}$$

where Ω_1 and Ω_2 are the Rabi frequencies of the corresponding transitions. When the resonance condition $\Delta_1 = \Delta_2$ is approximately satisfied, coherent population trapping (CPT) occurs, i.e., a specific coherence between the two lower states $|g_1\rangle$ and $|g_2\rangle$ forms a *dark state* given by

$$|\text{dark state}\rangle = \frac{\Omega_2}{\sqrt{|\Omega_1|^2 + |\Omega_2|^2}} e^{i\omega_{L1}t}|g_1\rangle - \frac{\Omega_1}{\sqrt{|\Omega_1|^2 + |\Omega_2|^2}} e^{i\omega_{L2}t}|g_2\rangle \ . \tag{3}$$

The dark state satisfies the condition

$$\langle e|\hat{H}_I|\text{dark state}\rangle = 0 \ , \tag{4}$$

i.e., the dark state does not interact with the applied laser field. Hence, CPT lasts until the relaxation process between the two lower states destroys the coherence described by Eq. (3). For a given detuning, $\Delta \equiv \Delta_1 - \Delta_2$, the probability of finding the atom in the dark state is determined by the optical Rabi frequencies and relaxation rate between the lower states, γ_g. If there is an energy level shift, due to the interaction with external electromagnetic fields, in one or both lower states, the difference of the shifts can be measured in the laser frequency difference $\omega_{L1} - \omega_{L2}$, when the resonance condition, $\Delta \equiv \Delta_1 - \Delta_2 = 0$ is satisfied. The resonance condition for CPT generation can be detected using any combination of fluorescence, transmission, and microwave emission (by the magnetic dipole associated with the dark state). When the optical signal is detected, no microwave cavity is required for implementation of the CPT-based atomic frequency standards. Fig. 2 shows the detected optical signals associated with the CPT-generation in a small ^{87}Rb vapor cell.

III. LIGHT SHIFT IN CPT-BASED FREQUENCY STANDARDS

In a practical atomic frequency standard, the choice of the lower states, e.g., the sub-states $|F=I\pm1/2, m_F=0\rangle$ in an alkaline atom's ground state, allows more transitions than the ones shown in Fig. 1(b) according to selection rules. The frequency component with frequency ω_{L1} (ω_{L2}) can also interact with induced electric dipole moment between the states $|e\rangle$ and $|g_2\rangle$ ($|g_1\rangle$) although it is detuned from resonance. When a single laser with frequency modulation (FM) is used for CPT-generation, every frequency component interacts with the induced electric dipole moment between the states $|e\rangle$ and $|g_1\rangle$ and the one between the states $|e\rangle$ and $|g_2\rangle$. The calculation has to take all these interactions into account. Typically, all the non-CPT-generating interactions have large detunings and low Rabi frequencies, so that they do not affect the CPT-generation process significantly. Therefore, it is justified that we consider the effects of the two CPT-generating interactions first, and treat the non-CPT-generating interactions as the perturbations. We will show that these non-CPT-generating interactions dominate the contributions to the light shift of the two lower states, $|g_1\rangle$ and $|g_2\rangle$, which are used to define the frequency standard. Based on these calculations, we propose a method to control or to ultimately eliminate the light shift.

III.1 LIGHT SHIFT FROM THE CPT-GENERATING INTERACTIONS

To calculate the effects of the two CPT-generating interactions we use the simplified system in Fig. 1(b). The density matrix equation for this system is

$$i\hbar\frac{d}{dt}\hat{\rho}=\left[\hat{H}_0+\hat{H}_I,\hat{\rho}\right]-\frac{1}{2}i\hbar\left[\hat{\Gamma}\hat{\rho}+\hat{\rho}\hat{\Gamma}\right] \tag{5}$$

where $\hat{H}_0$ is the Hamiltonian for the internal atomic states, $\hat{H}_I$ is given by Eq. (2), and $\hat{\Gamma}$ describes all the relaxation processes. Although the analytical solution for the steady state of this equation was given in the literature,[18] it is not trivial to interpret the physical meaning of the solution. The perturbation approximation was also used to solve this equation.[13] The results showed that the light shifts of the two lower states are the same for the dark state (with coherence shown in Eq. (3)) and for the case where there is no coherence between the lower states.

Here we solve Eq. (5) for a steady state solution in a closed form without further approximations. First the result is used for calculating the CPT under different parameter settings. Then this closed form result is used for the numerical calculation of the light shift difference between the lower states $|g_1\rangle$ and $|g_2\rangle$, which is the physical quantity measured in a frequency standard. We find out that the light shift difference between the lower states is much smaller in comparison with the one obtained without considering the coherence in Eq. (3). Fig. 3 shows an example of the light shift difference in the dark state vs. detuning with $2\Omega_1 = \Omega_2$. The result from the calculation without the presence of coherence is also shown in Fig. 3 for comparison. This small light shift is not a surprising result because the lack of the interaction between the dark state and the applied laser field, shown in Eq. (4), removes the light shift, at least to the lowest order. Therefore, we conclude that the light shift difference between the lower states from the two CPT-generating interactions is small enough, at least for the vapor cell type atomic frequency standards. However, the light shift from the non-CPT-generating interactions could be significant, and will be calculated in the next sub-section.

III.2 LIGHT SHIFT FROM THE NON-CPT-GENERATING INTERACTIONS

We start with the density matrix equation shown in Eq. (5) for the calculation of the light shift from the non-CPT-generating interactions. Here the interaction Hamiltonian only includes the non-CPT-generating interactions. Using perturbation approximations, one can eliminate the excited states in Eq. (5).[16] The equivalent density matrix equation for the ground states can be written as

$$i\hbar\frac{d}{dt}\hat{\rho}^G = \left[\left(\hat{H}_0^G + \delta\hat{H}^G\right), \hat{\rho}^G\right] - \frac{1}{2}i\hbar\left[\left(\hat{\Gamma}^G + \delta\hat{\Gamma}^G\right)\hat{\rho}^G + \hat{\rho}^G\left(\hat{\Gamma}^G + \delta\hat{\Gamma}^G\right)\right] \tag{6}$$

where the superscript G designates the operators to the ground states. Due to the existence of the non-CPT-generating interactions, in Eq. (6), the equivalent operators $\delta\hat{H}^G$ and $\delta\hat{\Gamma}^G$ represent the extra interactions and relaxations, respectively, among all the ground states. For each laser frequency component with an amplitude $\vec{E}_j$ and an angular frequency ω_{Lj}, we define the generalized Rabi frequency $\Omega_{m\mu}^j$ and detuning $\Delta_{m\mu}^j$ as

$$\Omega_{m\mu}^j \equiv \frac{1}{\hbar}\vec{E}_j \bullet \langle m|\hat{\vec{d}}|\mu\rangle \tag{7a}$$

$$\Delta_{m\mu}^j \equiv \omega_{Lj} - \frac{1}{\hbar}\left(E_m - E_\mu\right) \tag{7b}$$

where $\langle m|\hat{\vec{d}}|\mu\rangle$ is the induced electric dipole moment between the excited state |m> and ground state |μ>. Then corresponding matrix elements of operators $\delta\hat{H}^G$ and $\delta\hat{\Gamma}^G$ are given by

$$\langle\nu|\delta H^G|\mu\rangle = \frac{\hbar}{4}\sum_j\sum_m \frac{\Omega_{\nu m}^j\Omega_{m\mu}^j\Delta_{m\mu}^j}{{\Delta_{m\mu}^j}^2 + {\gamma_m}^2} + \frac{\hbar}{4}\sum_j\sum_{k\neq j}\sum_m \frac{\Omega_{\nu m}^k\Omega_{m\mu}^j\cos\left(\omega_{jk}t + \theta_{m\mu}^j\right)}{\sqrt{{\Delta_{m\mu}^j}^2 + {\gamma_m}^2}} \tag{8a}$$

$$\langle\nu|\delta\Gamma^G|\mu\rangle = \frac{1}{2}\sum_j\sum_m \frac{\Omega_{\nu m}^j\Omega_{m\mu}^j\gamma_m}{{\Delta_{m\mu}^j}^2 + {\gamma_m}^2} + \frac{1}{2}\sum_j\sum_{k\neq j}\sum_m \frac{\Omega_{\nu m}^k\Omega_{m\mu}^j\sin\left(\omega_{jk}t + \theta_{m\mu}^j\right)}{\sqrt{{\Delta_{m\mu}^j}^2 + {\gamma_m}^2}} \tag{8b}$$

$$\theta_{m\mu}^j \equiv \tan^{-1}\frac{\gamma_m}{\Delta_{m\mu}^j} \tag{8c}$$

where the sum of m is for all the excited states; sums of j and k are for all the frequency components. We write the non-oscillating terms and oscillating terms (with a frequency on the order of hyperfine splitting) separately in Eq. (8) because they have different effects on the ground states. In a typical vapor cell atomic frequency standard, the interaction strength, which is equivalent to the Rabi frequency, for each term in Eq. (8a) is much smaller than the relaxation rate among the ground states. Similarly, the rate of each term in Eq. (8b) is much smaller than the relaxation rate among the ground states. Therefore,the most important effect from Eq. (8) is the light shift, which is represented by the diagonal matrix element $\langle\nu|\delta H^G|\nu\rangle$. The

effect of the oscillating term in $\langle v|\delta H^G|v\rangle$ is averaged to zero while the non-oscillating term gives the light shift of state $|v\rangle$, which is similar to the one in Eq. (1). Although some of the oscillating terms in the off-diagonal matrix element $\langle v|\delta H^G|\mu\rangle$ can be in resonance with the transition used for frequency standards, their effects are still small due to the small interaction strength.

III.3 METHODS TO CONTROL OR ELIMINATE LIGHT SHIFT

From the above analysis, we demonstrate that one is able to control the total light shift in the CPT-based frequency standards by controlling the intensities and/or the frequencies of the non-CPT-generating frequency components.[19] For example, one can add one or more non-CPT-generating interactions by introducing extra frequency components with desired intensities and frequencies to suppress the total light shift in the system. When a single FM laser is used for CPT generation, it is very convenient to control the total light shift using the frequency modulation index. Fig. 4 shows the total light shifts vs. frequency modulation index with a single FM laser. The residual amplitude modulation (AM) could change the modulation index for zero total light shift slightly. Fig. 5 shows the light shifts vs. detuning with different frequency modulation indices.

All the above light shifts in Fig. 4 and Fig. 5 are calculated in an optically thin absorption medium. In a practical vapor cell atomic frequency standard, the absorption in the vapor is significant. If the vapor cell is filled with buffer gas, the atoms are localized due to the collision with the buffer gas molecules. Therefore, the light shift in the vapor cell varies with the position due to the absorption of different frequency components. The contribution to the detected signal also varies with the position in the vapor cell. Furthermore, these variations depend on the input laser beam intensity due to the balance between the CPT-generating process and the relaxation process among the ground states. The saturation effect is usually small. To compare the calculation with experimental results, we have to take all these factors into account. The possible exception is the case where one uses an FM laser with a small modulation index. The dominating contribution of the light shift in this case is from the laser carrier frequency that is not absorbed significantly within the vapor cell.

IV. EXPERIMENTAL RESULTS

We use a ^{87}Rb vapor cell in our experimental study of the light shift in the CPT-based frequency standard. We use the D_1-line for CPT-generation, as shown in Fig. 1(c). The laser source consists of either a pair of phase-locked diode lasers or a single diode laser with frequency modulation at 3.4 GHz. In the case of using an FM laser, the ±1st order sidebands are used for CPT-generation. The optical power ratio of these two sidebands is measured as $|J_{+1}/J_{-1}|^2 \approx 1.2$ for most of our measurements due to residual amplitude modulation. The averaged power in the ±1st order sidebands is used to estimate the frequency modulation index, which can readily reach 3. The laser beam is collimated and truncated just before it enters the vapor cell. The intensity variation across the beam is less than 10%, so that in the calculation we only consider the intensity variation in the vapor cell along the propagation direction of the laser beam.

Fig. 6 shows the measured light shift with a pair of phase-locked diode lasers. The laser frequencies are locked to the peak absorption corresponding to the excited state |F'=2>. Using the results in sub-section

III.2, we expect the positive light shift. To compare the experimental results with the calculation, the transmitted laser beam power is also measured to determine the absorption in the cell. By integrating the signal and the light shift along the absorption cell, the calculation of the total light shift is also shown in Fig. 6. The discrepancy between the calculation and the measurements is less than 5%.

Fig. 7 shows the measured light shifts using a single FM diode laser. We attribute the curvature of the light shift with a fixed modulation index to the factors discussed in sub-section III.3. It is clear from Fig. 7 that the light shift can be reduced or eliminated in the CPT-based vapor cell frequency standard by choosing the proper modulation index. The measured light shift can be used in a slow servo system to control the modulation index dynamically. Fig. (8) shows the light shift is suppressed using such a servo system with an incorrect initial modulation index setting.

We use a single FM diode laser to study the frequency stability of our CPT-based Rb vapor cell frequency standard. The frequency modulation index is either set or controlled to minimize the total light shift. The frequency stability is measured in comparison with an in-house ensemble consisting of two Agilent 5071A cesium-beam frequency standards. Fig. 9 shows the measured Allan deviations. Fig. 9 also shows the short-term frequency stability measurement ($1s \leq \tau \leq 4000s$) using a diode laser pumped Rb vapor cell frequency standard (not CPT-based) as a frequency reference. In this measurement, the frequency/phase noise from both the CPT-based Rb frequency standard and the reference contribute to the short-term stability $\sim 1.3\times10^{-12}\ \tau^{-1/2}$ and the flicker noise floor $\sim 1.4\times10^{-13}$. From the individual signal-to-noise measurements, we determine that the short-term stability is about the same for both the CPT-based Rb frequency standard and the reference. Removing the noise contribution from the reference, we expect the short-term stability to be $1\times10^{-12}\ \tau^{-1/2}$ and the flicker noise floor at $\sim 1\times10^{-13}$ for the CPT-based Rb frequency standard. The frequency drift of our CPT-based frequency standard is shown in Fig. 10. Apparently there is a frequency change with a period of 24 hours in our preliminary setup, especially during the weekends, when the temperature control of the building works in a different mode. This frequency change determines the Allan deviation for $\tau \cong 10{,}000s$, as shown in Fig. 9.

V. CONCLUSION

The calculation and measurement of light shift in CPT-based vapor cell frequency standards are presented. Our results show that the light shift could be significant. We present a general method[19] to suppress the light shift in CPT- based vapor cell frequency standards. We also present the short-term frequency stability measurement of our CPT-based rubidium vapor cell frequency standard using a single FM diode laser. By implementing the light shift control method, it is feasible to make a compact, moderately inexpensive CPT-based vapor cell frequency standard with good performance.

VI. ACKNOWLEDGMENTS

We are greatly indebted to Robin Giffard for beneficial discussions. We also gratefully acknowledge Jim Johnson and Ray Wong for their help in the project.

VII. REFERENCES

[1] G. Alzetta, A. Gozzini, L. Moi, and G. Orriols, Nuovo Cimento B **36**, 5 (1976).

[2] E. Arimondo and G. Orriols, Lett. Nuovo Cimento **17**, 333 (1976).

[3] G. Orriols, Nuovo Cimento **53**, 1 (1979).

[4] J. Thomas, S. Ezekiel, C. Leiby, R. Picard, and C. Willis, Opt. Lett. **6**, 298 (1981).

[5] J. Thomas, P. Hemmer, S. Ezekiel, C. Leiby, R. Picard, and C. Willis, Phys. Rev. Lett. **48**, 867 (1982).

[6] A. Aspect, E. Arimondo, R. Kaiser, N. Vansteenkiste, and C. Cohen-Tannoudji, Phys. Lett. **61**, 826 (1988).

[7] M. O. Scully, Phys. Rev. Lett. **67**, 1855 (1991).

[8] M. O. Scully, Phys. Rep. **219**, 191 (1992).

[9] E. Arimondo, Prog. Opt. **XXXV**, 257 (1996), and the references therein.

[10] S. Brandt, A. Nagel, R. Wynands, and D. Meschede, Phys. Rev. A **56**, R1063 (1997).

[11] P. Hemmer, V. Natoli, M. Shahriar, B. Bernacki, H. Lamela-Rivera, S. Smith, and S. Ezekiel, in *Proceedings of the 1987 IEEE International Frequency Control Symposium*, p. 42.

[12] N. Cyr, M. Tetu, and M. Breton, IEEE Trans. Instrum Meas. **42**, 640 (1993).

[13] J. Vanier, A. Godone, and F. Levi, Phys. Rev. **A58**, 2345 (1998).

[14] See, for example, C. Cohen-Tannoudji, J. Dupont-Roc, and G. Grynberg, *Atom-Photon Interactions*, (John Wiley & Sons, New York 1992).

[15] See, for example, L. Schiff, *Quantum Mechanics*, (McGraw-Hill Book Company, New York 1968).

[16] See, for example, W. Happer, Rev. of Mod. Phys. **44**, 169 (1972), and the references therein.

[17] C. Cohen-Tannoudji, in *Frontiers of Laser Spectroscopy*, R. Balian, S. Haroche, and S. Liberman, eds. (North-Holland Publishing Company, Amsterdam 1977).

[18] See, for example, R. Brewer and E. Hahn, Phys. Rev. A **11**, 1641 (1975).

[19] U. S. Patent pending.

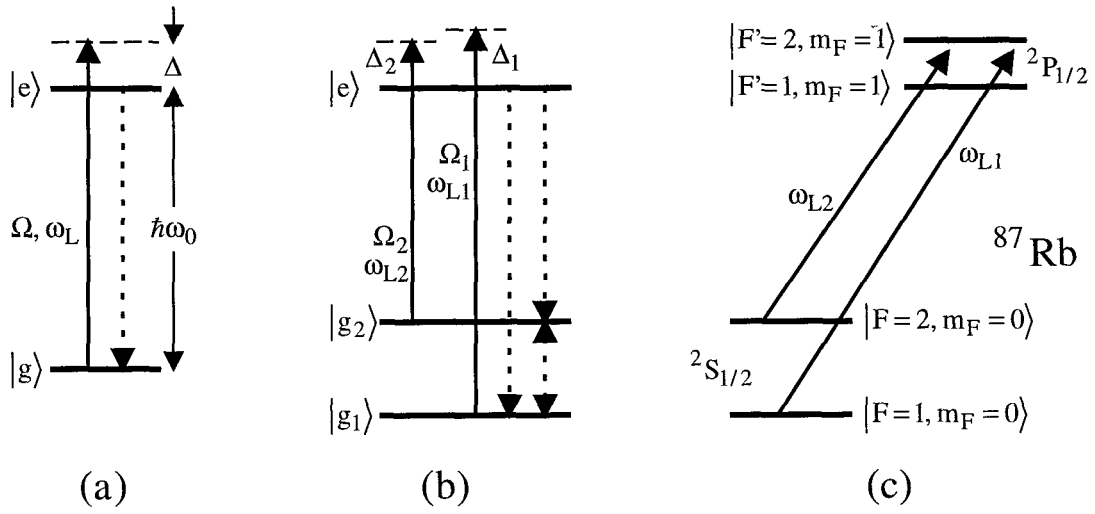

Figure 1. (a) A two-energy-level atom interacting with a single frequency laser field for calculation of light shift. (b) A three-energy-level atom interacting with a dual-frequency laser field for CPT-generation. (c) Part of the energy levels in a ^{87}Rb atom for implementing a CPT-based frequency standard. Only two laser frequency components driving the CPT-generating interactions are shown explicitly. Relaxation processes are presented by dashed lines in (a) and (b), but are not shown in (c) explicitly.

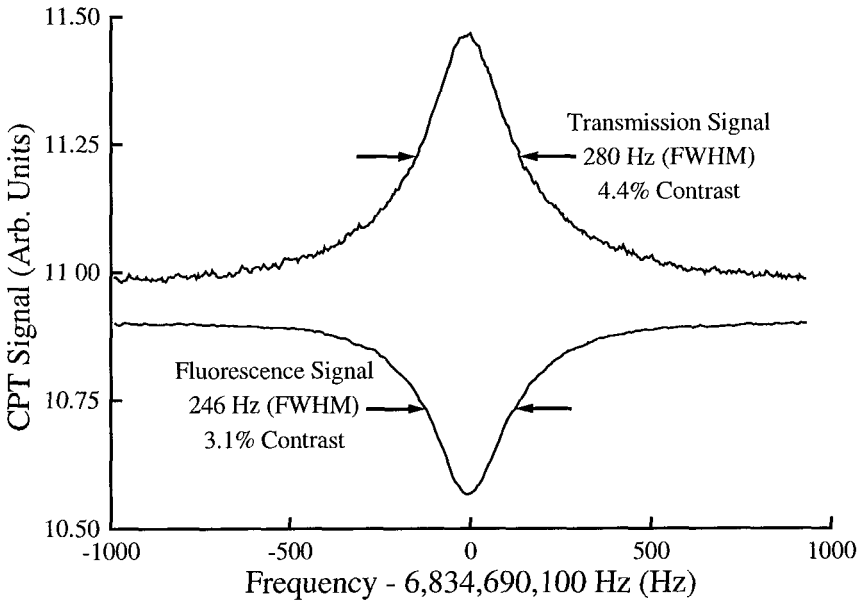

Figure 2. Transmission and fluorescence signals of coherent population trapping in a ^{87}Rb vapor cell. A single FM laser is used with frequency modulation index about 2.2. A solid angle of ~1.2 steradian is covered by the photo-detector for fluorescence detection.

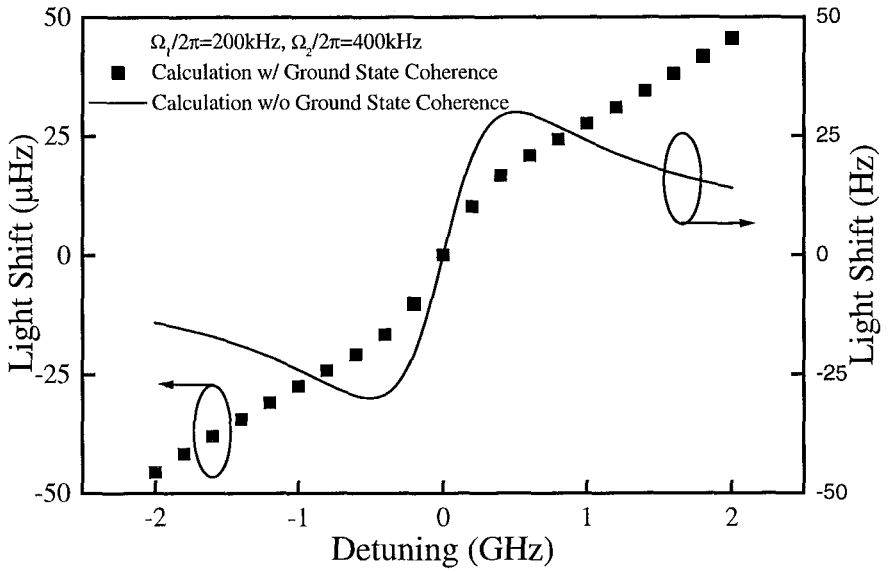

Figure 3. Calculated light shifts from CPT-generating interactions.

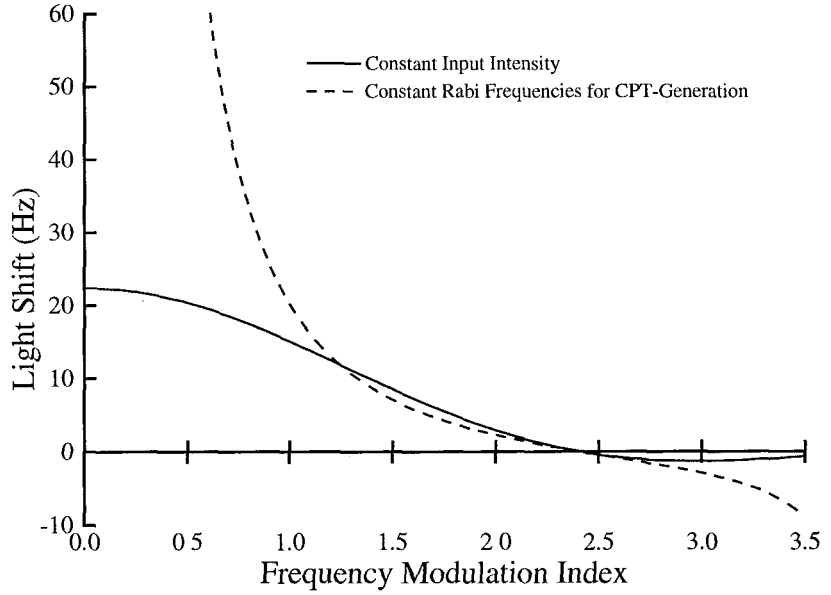

Figure 4. Calculated light shifts vs. frequency modulation index. The Rabi frequencies for both CPT-generating interactions are 200 kHz when FM index equals to 2.45.

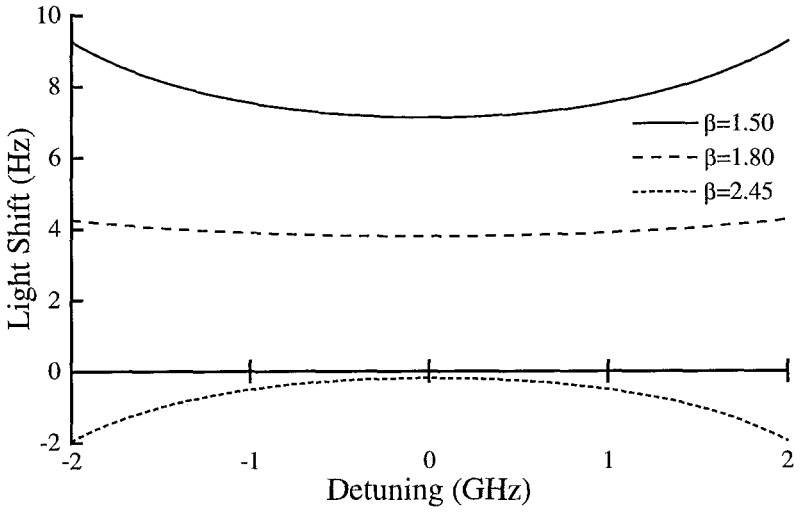

Figure 5. Calculated light shifts vs. detuning. The Rabi frequencies are 200 kHz for both CPT-generating interactions.

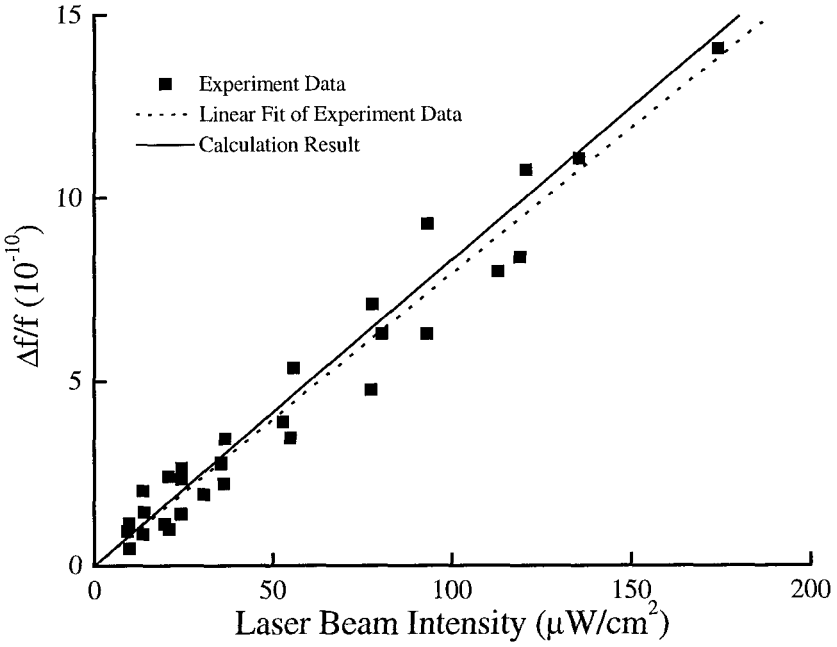

Figure 6. Light shifts in a CPT-based ^{87}Rb vapor cell frequency standard using a pair of phase-locked diode lasers.

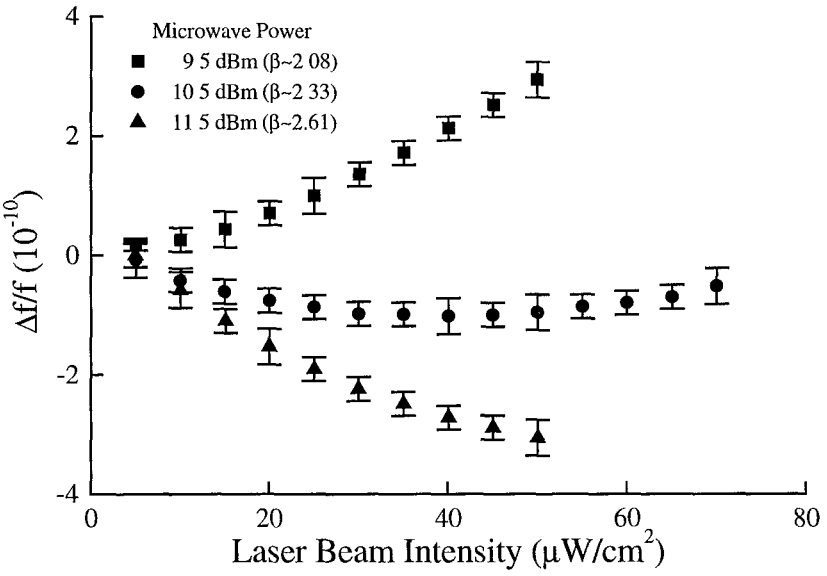

Figure 7. Light shifts in a CPT-based ^{87}Rb vapor cell frequency standard with an FM laser.

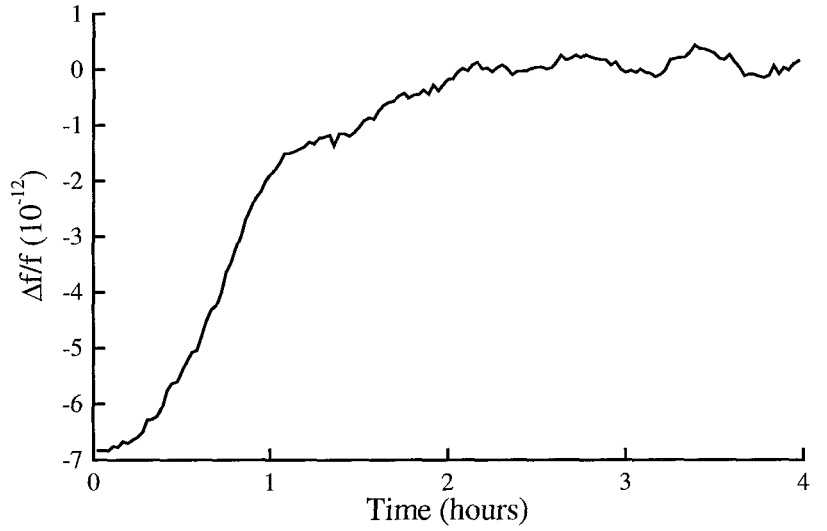

Figure 8. Correction of the initial offset of frequency modulation index.

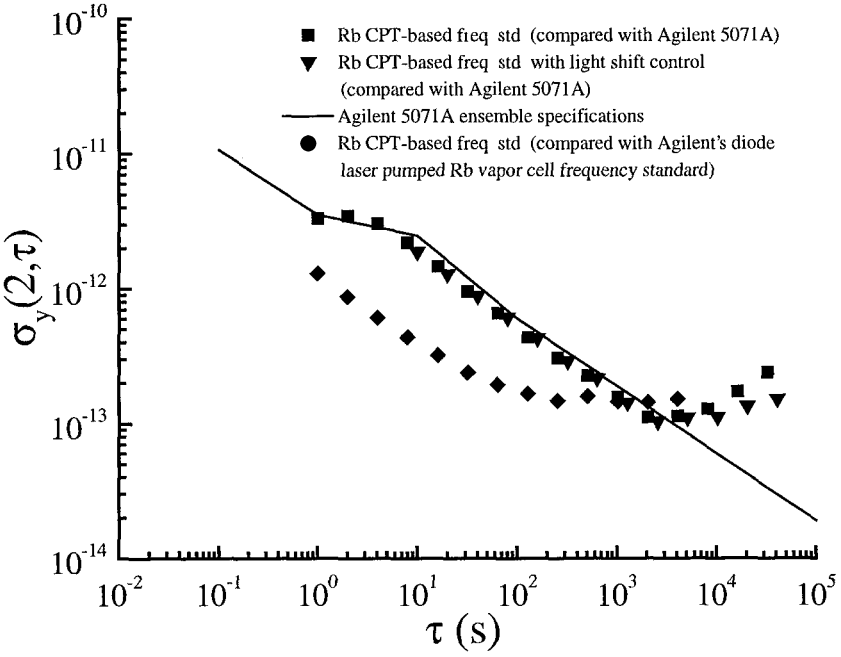

Figure 9. Short-term stability measurements of a CPT-based ^{87}Rb vapor cell frequency standard.

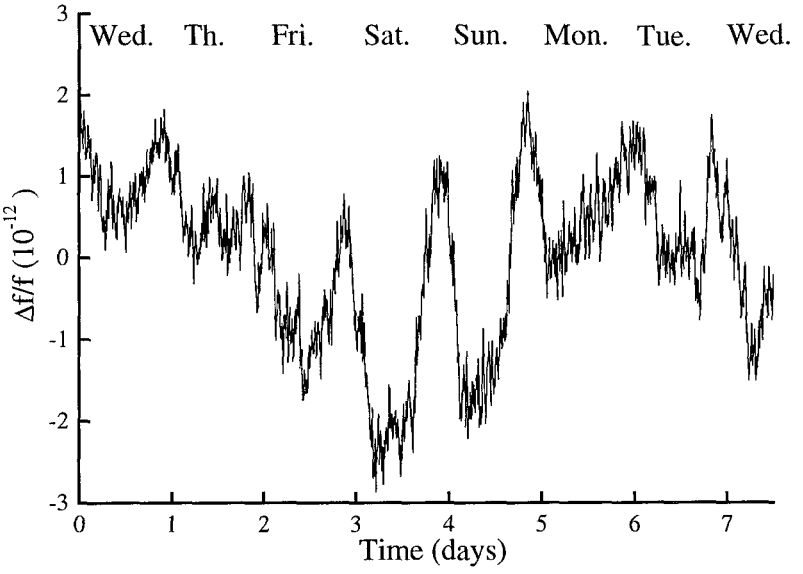

Figure 10. Relative frequency drift of a CPT-based ^{87}Rb vapor cell frequency standard.

Questions and Answers

ROBERT LUTWAK (Datum): When you servo the microwave power to eliminate the light shift, what do you servo to? To what are you leveling that signal?

MIAO ZHU: Do you mean what I servo to or where did I do the servo?

LUTWAK: What is the error signal that determines the TR microwave modulation as causing a non-zero light shift?

ZHU: You can modulate it or have it at a low frequency and that can drive that signal from there.